Hippocampal growth hormone modulates relational memory and the dendritic spine density in CA1

Kamilla G. Haugland,[1] Anniken Olberg,[1] Andreas Lande,[1] Kirsten B. Kjelstrup,[1,2] and Vegard H. Brun[1,2]

[1]Department of Clinical Medicine, University in Tromsø—The Arctic University of Norway, 9019 Tromsø, Norway; [2]University Hospital of North Norway, 9019 Tromsø, Norway

Growth hormone (GH) deficiency is associated with cognitive decline which occur both in normal aging and in endocrine disorders. Several brain areas express receptors for GH although their functional role is unclear. To determine how GH affects the capacity for learning and memory by specific actions in one of the key areas, the hippocampus, we injected recombinant adeno-associated viruses (rAAVs) in male rats to express green fluorescent protein (GFP) combined with either GH, antagonizing GH (aGH), or no hormone, in the dorsal CA1. We found that aGH disrupted memory in the Morris water maze task, and that aGH treated animals needed more training to relearn a novel goal location. In a one-trial spontaneous location recognition test, the GH treated rats had better memory performance for object locations than the two other groups. Histological examinations revealed that GH increased the dendritic spine density on apical dendrites of CA1, while aGH reduced the spine density. GH increased the relative amount of immature spines, while aGH decreased the same amount. Our results imply that GH is a neuromodulator with strong influence over hippocampal plasticity and relational memory by mechanisms involving modulation of dendritic spines. The findings are significant to the increasing aging population and GH deficiency patients.

[Supplemental material is available for this article.]

The hippocampal network is essential for the acquisition and organization of relational memory (Eichenbaum 2017). The dense *N*-methyl-D-aspartate (NMDA) receptor distribution on hippocampal synapses allows their strengths to be quickly altered, making the network ideal for memory formation (Moser et al. 1994; Shimizu et al. 2000; Brun et al. 2001; Nakazawa et al. 2004). Numerous neuromodulators influence the plasticity of the hippocampus and modify the neural circuits (Cobb and Lawrence 2010). While research on synaptic plasticity has focused on common neuromodualtors like acetylcholine, noradrenaline, serotonin, and dopamine (Palacios-Filardo and Mellor 2018), the potential influence of growth hormone (GH) is less explored.

Growth hormone is commonly known as a peptide hormone secreted by the pituitary into the bloodstream to regulate somatic growth, but can also function as a neuromodulator in the central nervous system (Nyberg 2000; Åberg et al. 2006). Receptors for GH are robustly expressed throughout the central nervous system, including the hippocampus (Burton et al. 1992; Lobie et al. 1993, 2000; Nyberg 2000). Although systemic GH can cross the blood–brain barrier and enter the brain (Pan et al. 2005), GH is also produced locally in the hippocampus (Donahue et al. 2006), suggesting a self-regulating function. One of the first indications of an autonomous GH regulation in the hippocampus came from observations with the GH-deficient Ames dwarf mice. With impaired GH secretion from the anterior pituitary, the Ames dwarf mice retain compensatory higher levels of GH levels in the hippocampus, making their memory significantly improved (Sun et al. 2005). Furthermore, there is evidence that GH can affect memory systems

through hippocampal NMDA and α-amino-3-hydroxy-5-methyl-4-isoxazole propionic acid (AMPA) receptor signaling (Le Greves et al. 2002; Ramis et al. 2013; Studzinski et al. 2015). These receptors are key components of long-term potentiation (LTP), which in turn can influence dendritic spine density (Matsuzaki 2007). However, the evidence that directly relates the behavioral outcome of GH to the possible underlying morphological changes is still missing.

Although several reports argue for a role of GH in learning and memory (Nyberg and Hallberg 2013; Ashpole et al. 2015), few have tried to decipher the involved neurobiological mechanisms. There are studies showing cognitive improvements after GH therapy in patients diagnosed with GH deficiency (Deijen et al. 1998; Sathiavageeswaran et al. 2007; Nieves-Martinez et al. 2010). In animals, systemic administration of GH or the GH secretagogue ghrelin improves spatial memory (Schneider-Rivas et al. 1995; Diano et al. 2006; Grönbladh et al. 2013), while spontaneous dwarf rats with a deficient version of the GH-gene show impaired memory performance in the Morris water maze task (Li et al. 2011). Conflicting reports describe improved spatial memory after GH receptor knockout (Basu et al. 2017) and ghrelin receptor knockout (Albarran-Zeckler et al. 2012), as well as impaired memory after systemic ghrelin administration (Zhao et al. 2014). An explanation for these various results after GH manipulation could be that *systemic* GH has diverse effects in different kinds of tissues

Corresponding author: vegard.h.brun@uit.no
Article is online at http://www.learnmem.org/cgi/doi/10.1101/lm.050229.119.

(Sun and Bartke 2014). Many reports make claims about cognitive effects based on systemic GH manipulations, but the observed behavior could result from peripheral stimulation, including alterations in muscle strength, locomotor activity or other abilities. Consequently, to reveal the function of GH specifically in the hippocampus, we performed targeted manipulations of GH in the cornu ammonis (CA)1 in vivo to see if this was enough to produce both behavioral and morphological changes.

Results

To investigate the role of GH as a neuromodulator in learning and memory, we injected recombinant adeno-associated viruses (rAAVs) in the dorsal hippocampus to express GH, antagonizing GH (aGH) or green fluorescent protein (GFP) only (control). The antagonizing GH was a muted GH with the exchange of a single amino acid in the GH-gene (Chen et al. 1990, 1991). All the rAAVs contained sequences for GFP for visual verification of the transfections. The viral constructions were similar for the GH modulated groups, AAV-CMV-GH-IRES-GFP or AAV-CMV-aGH-IRES-GFP, respectively. The control groups were either unoperated or transfected with rAAV expressing GFP only (AAV-CMV-IRES-GFP). The animals that received virus were allowed 3 wk of viral incubation time before the memory performance was tested in hippocampal-dependent memory tasks (Fig. 1A).

Injections sites and transfected neurons in the dorsal hippocampus

Injections were made bilaterally at four antero-posterior sites with different proximal-distal coordinates, to cover large parts of the dorsal hippocampal CA1 (Fig. 1B). The viral load was calibrated to avoid excitotoxic lesions and epilepsy, which occurred in pilot experiments in some animals receiving substantially higher viral loads, in particular with the GH virus. In the presented data, we observed no convulsive seizures and found no signs of lesions in Nissl stained brain sections other than the expected minor mechanic lesions from the surgery in all groups. All animals had successful viral transfection in the hippocampus verified by the presence of GFP expression (Fig. 1C; $n = 8$ for GH, $n = 8$ for aGH, $n = 13$ for control), although the amount of GFP expression varied. Transfected neurons with GFP expression were mainly observed in CA1 pyramidal neurons, but also some CA3 pyramidal neurons and dentate gyrus (DG) granule cells were transfected. In addition, GFP was also seen in some nonpyramidal cells, especially in stratum radiatum in close proximity to injections in CA1 (Supplemental Fig. 1).

Growth hormone increases activation of p-Stat5

The GH peptide has properties to bind and activate the GH receptor in the hippocampus (Burton et al. 1992). The function of the GH receptor can be modulated by changing the availability and structure of the GH ligand (Birzniece et al. 2009), which is reflected by the receptor activation. By calculating the amount of phosphorylated Signal transducer and activator of transcription 5 (p-Stat5), changes in GH-induced receptor activation are observable (Furigo et al. 2017). To validate that our viral treatments affected GH receptor activation, we used immunohistochemistry for p-Stat5 combined with 4′,6-Diamidino-2-Phenylindol (DAPI) as a nuclear staining (Fig. 2A–F). This allowed comparison of the amount of p-Stat5 cells in the injection area of the hippocampus. Viral treatment significantly elevated the amount of p-Stat5 staining in the GH group (Fig. 2B,E, one-way ANOVA $F_{(2,36)} = 6.34$, $P = 0.004$, post-hoc Bonferroni t-test $t_{(36)} = 2.59$, $P = 0.013$). However, the amount of p-Stat5 positive cells in the aGH group was not significantly lower than in controls ($t_{(36)} = 0.70$, $P = 0.48$). Increasing the viral load fivefold in pilot experiments similarly failed to suppress p-Stat5 counts significantly below control animals, suggesting a floor effect (Supplemental Fig. 3).

Growth hormone increases dendritic spine density in CA1 stratum radiatum

As systemic ghrelin administration has been shown to increase the spine density in the hippocampus (Diano et al. 2006), and GH
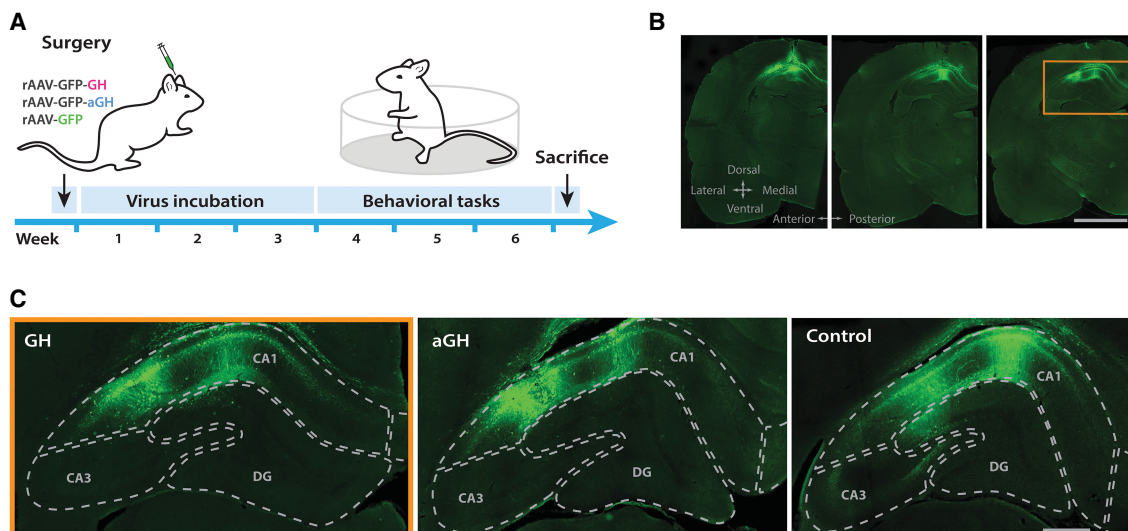
Figure 1. Experimental time line and illustration of viral transfection. (A) Rats received recombinant adeno-associated virus (rAVV) injections with either growth hormone (GH), antagonizing GH (aGH), or green fluorescent protein (GFP) only (control). After three weeks of virus incubation, behavioral assessments began. (B) Injection sites in dorsal hippocampus are shown by GFP labeling in a representative animal (GH) in coronal sections of the right hemisphere at different anteroposterior levels. Scale bar 200 µm. (C) Representative distribution of GFP labeled cells in the hippocampus of a GH, aGH, and control animal. The GFP labeling showed transfected cells in CA1, but also some in CA3 and DG. *Left* panel in C is a close-up from the most posterior section in B (orange frame). Scale bar 50 µm.
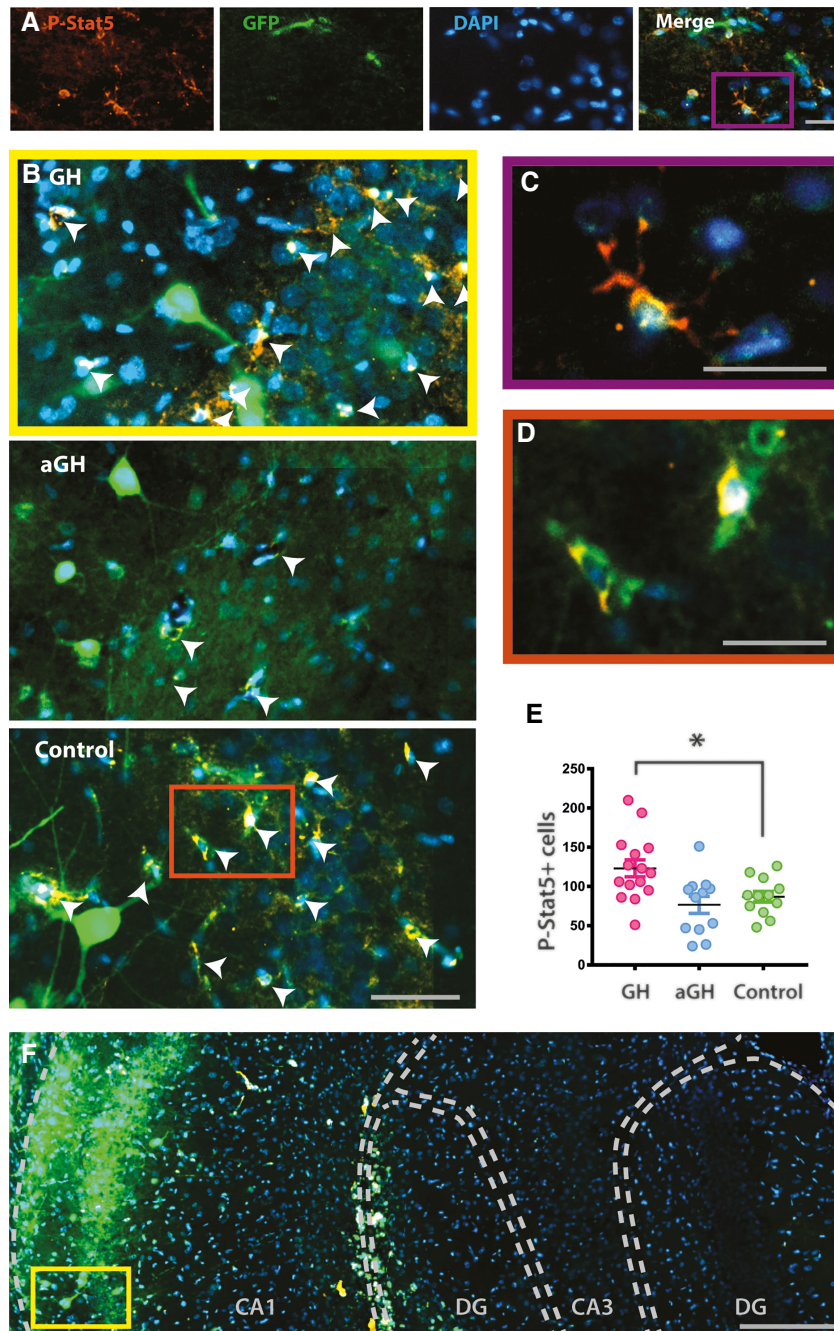
Figure 2. Growth hormone (GH) receptor activation quantified by p-Stat5 in the hippocampus. (*A*) Examples of p-Stat5 signal (red), green fluorescent protein (GFP; green), DAPI (blue), and merged in a control animal. Scale bar 20 μm. (*B*) Representative sections from a GH treated animal (close-up from illustration in F, yellow frame), aGH treated animal, and control animal, with p-Stat5, GFP, and DAPI. Scale bar 50 μm. (*C*) Illustration of a p-Stat5 positive DAPI cell, close-up from the merged illustration in *A* (purple frame). Scale bar 20 μm. (*D*) Illustration of two p-Stat5 positive, GFP positive DAPI cells (merged green and red becomes yellow), close-up from the example control animal in *B* (orange frame). Scale bar 20 μm. (*E*) The amount of p-Stat5 in the GH, aGH, and control group: GH significantly increased the number of p-Stat5 positive DAPI cells (ANOVA $F_{(2,36)} = 6.33$, $P = 0.004$, *t*-test $P = 0.013$), but p-Stat5 in the aGH group was not significantly lower than in controls. (*F*) Cross section overview of hippocampus from the GH treated animal in B, showing p-Stat5, GFP, and DAPI. GFP labeling is seen most dense in injection area CA1. Scale bar 200 μm.

apical dendrites from pyramidal cells in CA1 were visualized by the GFP expression (Fig. 3A,B), and only spines on apical dendrites in the stratum radiatum were included in our analysis ($n = 22$ putative pyramidal cells in four aGH treated animals, $n = 8$ in three control animals, and $n = 15$ in three GH treated animals). Average spine density was calculated for each putative neuron before a Jonckheere–Terpstra test for ordered alternatives showed significant groups differences in the expected order (Fig. 3C), with the lowest spine density (0.85 ± 0.04 spines/μm) in the aGH group, 1.00 ± 0.04 spines/μm in controls and highest spine density (1.26 ± 0.07 spines/μm) in the GH group ($T_{JT} = 530$, $P < 0.001$). The same group order was also significant when we did the statistical analysis at animal level (aGH 0.89 ± 0.06, control 1.09 ± 0.04, and GH 1.29 ± 0.10; $T_{JT} = 32$, $P < 0.005$). Pairwise group comparisons at neuron level revealed that the GH treatment increased spine density compared to the control (Mann–Whitney *U*-test, $Z = 2.58$, $P < 0.05$) and that aGH lowered the spine density compared to the control ($Z = 1.92$, $P < 0.05$).

Spine shapes varies over a continuum of morphologies, and can be categorized as filopodia, immature or mature spines. If GH has a function in maintaining learning capacity, it could specifically increase filopodia or immature spines which are associated with plasticity and learning capacity (Berry and Nedivi 2017; Ozcan 2017). We therefore categorized the counted spines blindly into filopodia-like, immature or mature and analyzed them at a neuron level ($n = 15$ GH, $n = 22$ aGH, $n = 8$ control). We found that the percentage of immature spines was increased in the GH group as compared to controls (Fig. 3D, one-way ANOVA $F_{(2,42)} = 23.7$, $P < 0.001$, post-hoc contrast $t_{(42)} = 6.36$, $P = 0.036$), and decreased in the aGH group ($t_{(42)} = 11.4$, $P < 0.001$). An opposite effect was observed for mature spines, GH treatment decreased the relative amount of mature spines (one-way ANOVA $F_{(2,42)} = 21.3$, $P < 0.001$, $t_{(42)} = 11.84$, $P = 0.003$), while aGH treatment increased the relative amount of mature spines ($t_{(42)} = 8.12$, $P = 0.019$) as compared to controls. The relative amount of filopodia-like spines was similar in all three groups (one-way ANOVA $F_{(2,42)} = 0.79$, $P = 0.46$).

Hippocampal growth hormone receptor antagonism disrupts memory

To determine if hippocampal GH modulation affects hippocampal-dependent long-term memory processes, we trained the rats in the water maze over five subsequent days. The rats learned to

application on CA1 hippocampal slices increases excitatory synaptic transmission (Molina et al. 2012), we wanted to see if the local GH manipulation in our rats affected the spine density. Spines on
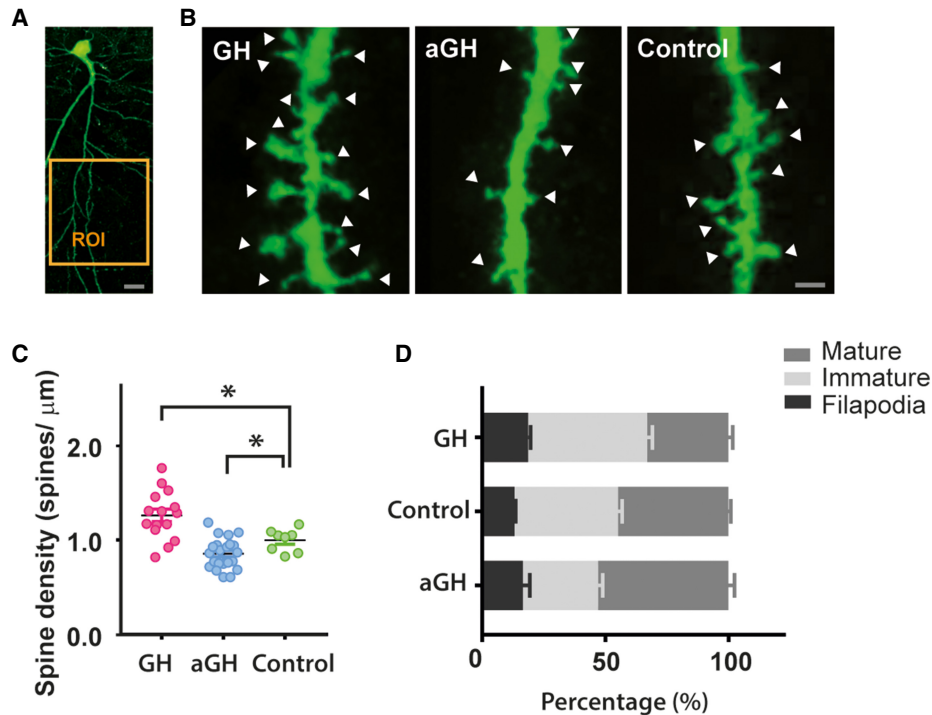
Figure 3. Growth hormone (GH) increases the density of dendritic spines in CA1, while antagonizing GH (aGH) reduced the spine density. (*A*) Example of green fluorescent protein (GFP) labeled pyramidal cell in CA1. Spines 100–200 μm from the soma (region of interest [ROI]; orange frame) on apical dendrites were used in the analysis when the entire neuron was traceable. Scale bar 20 μm. (*B*) Representable segments of dendrites with spines in the GH, aGH, and control group, respectively. Scale bar 1 μm. (*C*) Average spine density for individual spine segments (each dot) was highest in GH treated animals, while aGH had lower spine density than the other group ($n = 15$ in three GH treated animals, $n = 22$ spine counted regions in four aGH animals, and $n = 8$ in three control animals; Jonckheere–Terpstra test, JT = 32, $P = 0.003$). (*D*) The distribution of spine morphologies (filipodia, immature or mature) shown in percentages. GH animals had more immature spines than controls (one-way ANOVA $F_{(2,42)} = 23.7$, $P < 0.001$, *t*-test, $P = 0.036$) while aGH had less immature spines than controls (*t*-test, $P < 0.001$). On the other hand, aGH increased the percentage of mature spines (one-way ANOVA $F_{(2,42)} = 23.7$, $P < 0.001$, *t*-test, $P = 0.019$) while mature spines were decreased after GH treatment (*t*-test, $P = 0.003$).

find a submerged platform 1 cm under opaque water using distal landmarks in the room. The first trial of each day started as a probe trial with the platform inaccessible for 60 sec to reveal a potential search bias. To reduce the number of animals needed in the experiments, our control group included data from seven animals from pilot experiments that used the same GFP-expressing AAV virus in fivefold higher dose than used for all other animals. The high titer control group ($n = 7$) did not differ from the normal titer control animals ($n = 6$) on any of the water maze probe tests (two-way ANOVA showed no Group × Zone interaction on day 6, 12, 13, or 14, P value range 0.20–0.87).

We found successful learning curves for all the three groups during the 5 d of training (Fig. 4A, repeated measures ANOVA $F_{(4,104)} = 40.97$, $P < 0.001$), but no group difference (ANOVA Day × Group interaction $F_{(8,104)} = 1.76$, $P = 0.09$). As even hippocampus lesioned rats can learn this task after repeated training, we also looked for early effects of the treatment. A subanalysis of the first day of water maze training showed that the slightly shorter escape latencies of the GH group were not significantly different from the other groups (Fig. 4A, one-way ANOVA of Day 1 Latencies $F_{(2,26)} = 1.42$, $P = 0.26$). After the 5 d of training, memory for the target platform location was tested on a probe test with the platform unavailable. There was a significant Zone × Group interaction (Fig. 4B; two-way ANOVA ($F_{(6,78)} = 3.59$, $P = 0.003$). One-way ANOVA of time in the platform zone showed a significant group difference ($F_{(2,26)} = 4.61$, $P < 0.019$). Subsequent orthogonal comparisons showed that GH and control groups performed at the same level ($t_{(26)} = 0.34$, n.s.), and that the aGH group spent less time in the

platform zone compared to the other two groups ($t_{(26)} = 2.95$, $P = 0.004$). Examples of typical swim paths are shown in Figure 4C.

To reveal a possible benefit of GH treatment, we hypothesized that changing the goal location for these rats, which already knew the procedural parts of the task, could uncover group differences in flexible relational learning. After a 6-d break, we changed the platform location to the opposite quadrant in the water maze and trained the same animals for two more days, 4 × 4 trials (Fig. 4D). At the start of reversal training, all groups had a similar bias toward the old platform location, (Fig. 4E, ANOVA Group × Zone interaction $F_{(6,78)} = 0.48$, n.s.). However, after 1 d of reversal training only the control rats and the GH treated rats spent more time in the platform zone than the aGH rats on the 60 sec probe test (Fig. 4F, two-way ANOVA Zone × Group interaction $F_{(6,78)} = 2.54$, $P < 0.05$; one-way ANOVA of time in target zone $F_{(2,26)} = 3.64$, $P < 0.05$, subsequent orthogonal comparisons showed no difference between GH and control ($t_{(26)} = 0.5$), n.s.), but aGH searched significantly less in the new platform zone than the other two groups ($t_{(26)} = 2.69$, $P < 0.01$). Interestingly, the aGH rats tended to search for the old platform location on the first test (day 13; note the color plot in Fig. 4F), although a Day × Group interaction on escape latencies was not observed (Fig. 4D, repeated measures ANOVA $F_{(2,25)} = 1.30$, n.s.). After the second day of reversal training, on the final probe test on day 14, all the groups showed that they had learned the task (Fig. 4G, significant effect of Zone $F_{(3,75)} = 22.98$, $P < 0.001$, but no Zone × Group interaction, $F_{(3,75)} = 1.25$, $P > 0.25$). Interestingly, the GH group now tended to dwell at both the new and the old platform locations (color plot in Fig. 4G). This behavior
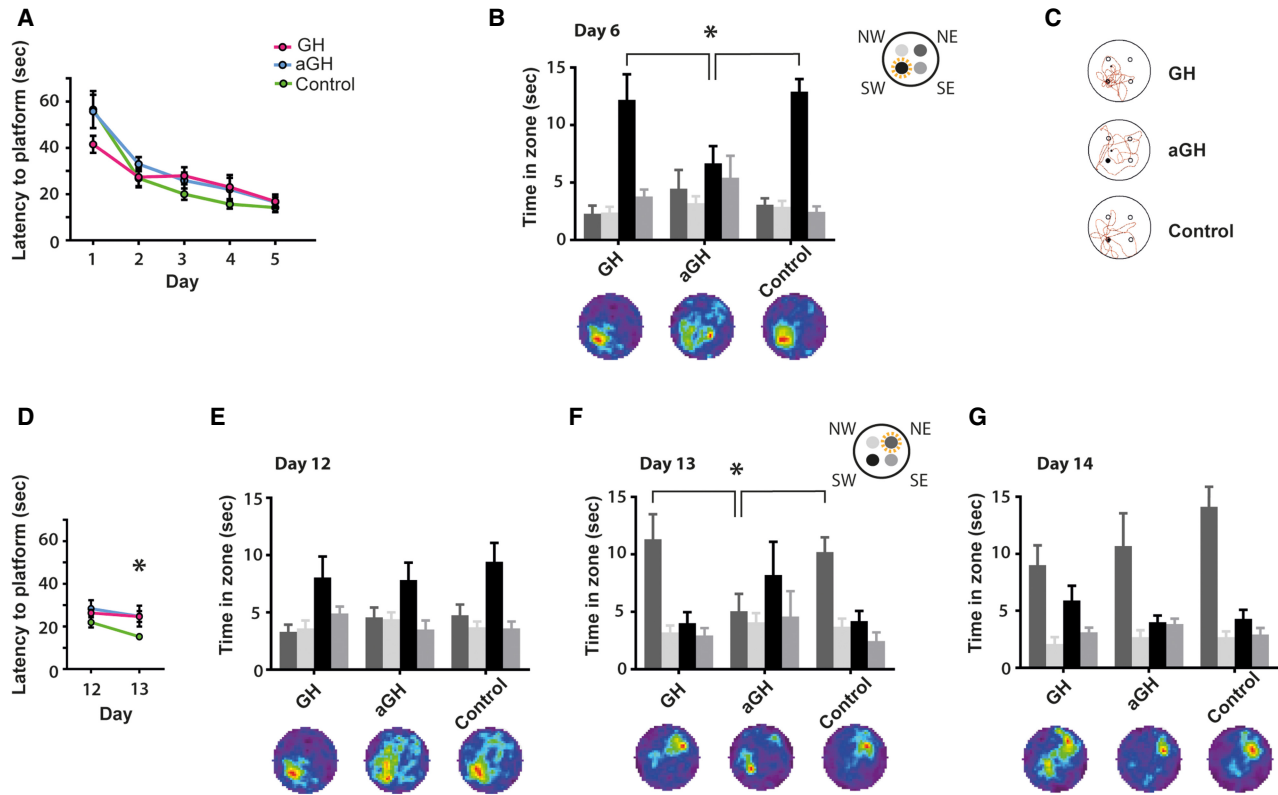
Figure 4. Antagonizing growth hormone (aGH) in the dorsal hippocampus impairs memory in the water maze. (*A*) Latencies on initial training on day 1–5 to the target zone southwest (SW). $n = 8$ GH, $n = 8$ aGH, $n = 13$ controls. (*B*) Search patterns during the 60 sec probe trial on day 6: The histogram of time spent in four 50 cm diameter zones shows that the aGH treated animals spent less time in the platform zone than the GH treated and control animals (post-hoc orthogonal comparisons of aGH versus the two other groups, $t_{(26)} = 2.95$, $P < 0.004$). The *upper right* figure illustrates the zones; the target zone SW (yellow dotted circle), southeast (SE), northeast (NE), and northwest (NW). The occupancy maps below illustrate the average search pattern for each group. Red in the occupancy maps indicates the most time spent in that location, while dark blue indicates the least time spent in that part of the water maze. (*C*) Representative individual swim paths on probe test day 6 for the GH, aGH, and control group, respectively. (*D*) Latencies during reversal training, same animals as in *A*. (*E*) Search pattern for probe trial on day 12, at initiation of reversal training. All groups remembered the platform location SW equally (two-way ANOVA effect of Zone × Group $F_{(6,78)} = 0.48$, $P = 0.82$). Occupancy maps below illustrate that all groups spent the most time in the SW zone. (*F*) Probe trial on day 13, the GH and control animals spent more time near the new NE goal location than aGH (post-hoc orthogonal comparisons of aGH vs the two other groups $t_{(26)} = 2.69$, $P = 0.006$). The aGH group tended to search for the old platform location. The *upper right* figure illustrates the platform zones with the new target zone NE (yellow dotted circle). Occupancy maps below illustrates that GH and control animals spent the most time in NE zone, while aGH animals spent the most time in the SW zone. (*G*) After 2 d of training, on day 14, all groups searched for the novel platform location (two-way ANOVA $F_{(3,75)} = 22.98$; $P < 0.001$, but no Zone × Group interaction $P > 0.25$). Occupancy maps below illustrate that all the groups spent the most time in the NE zone, although the GH animals also spent time searching for the old goal location (SW).

could express that GH treated rats are fast switchers of strategy when the platform position is made unavailable.

The GH transfections did not seem to cause any unspecific somatic or locomotor effects, unlike systemic GH administration (Sun and Bartke 2014). In particular, we observed no differences in weight gain (ANOVA $F_{(2,34)} = 0.67$, n.s.), swimming speed (ANOVA $F_{(5,120)} = 1.07$, n.s.), or path length (ANOVA $F_{(5,120)} = 0.43$, n.s.; Supplemental Fig. 2). To verify that our results in the water maze were due to spatial memory deficits, and not motor or balance impairments interfering with the rats' ability to climb onto the platform, all the animals completed a balance beam test with no observed impairments (none fell off in either group during the 60 sec test).

Growth hormone enhances spontaneous location recognition

If GH is beneficial to hippocampal function, multiple-trial water maze learning may be too complex to reveal the effects, as procedural and relational learning happens in parallel. We therefore ex-

posed the rats to several versions of a memory task that only require a single learning trial, the spontaneous location recognition (SLR) task. In the simplest version we made of this task (Fig. 5A), the animals were first presented with two identical objects in two pseudorandomized corners of a familiar box. After a 3 h delay, two identical copies were accessible, one in the old corner (familiar location), whereas the other was placed in a new corner (novel location). Rats naturally tend to explore the displaced object more. In the test phase, all the groups of animals spent more time exploring the novel object location (Fig. 5B upper panel; 29.4 ± 2.5 sec, 32.0 ± 4.5 sec, and 32.9 ± 3.6 sec in the GH, aGH, and control group), compared to the familiar location (20.4 ± 1.8 sec, 18.7 ± 3.9 sec, and 22.4 ± 1.5 sec, respectively; paired t-tests, $t_{(7)} = 3.78$; $t_{(7)} = 3.41$; $t_{(11)} = 2.50$; $P < 0.05$ for all). To ensure no bias in our data, all four corners of the arena were used in a pseudorandomized order (Fig. 6A–C). Object exploration was independent of the corners used during the sample phase, indicating no bias to a certain corner in the box (Fig. 6C; one-way ANOVA of object exploration in all four corners on the first sample trial, before 3 h delay $F_{(3,54)} = 0.64$ n.s.). Neither did we see a bias toward corner on the second
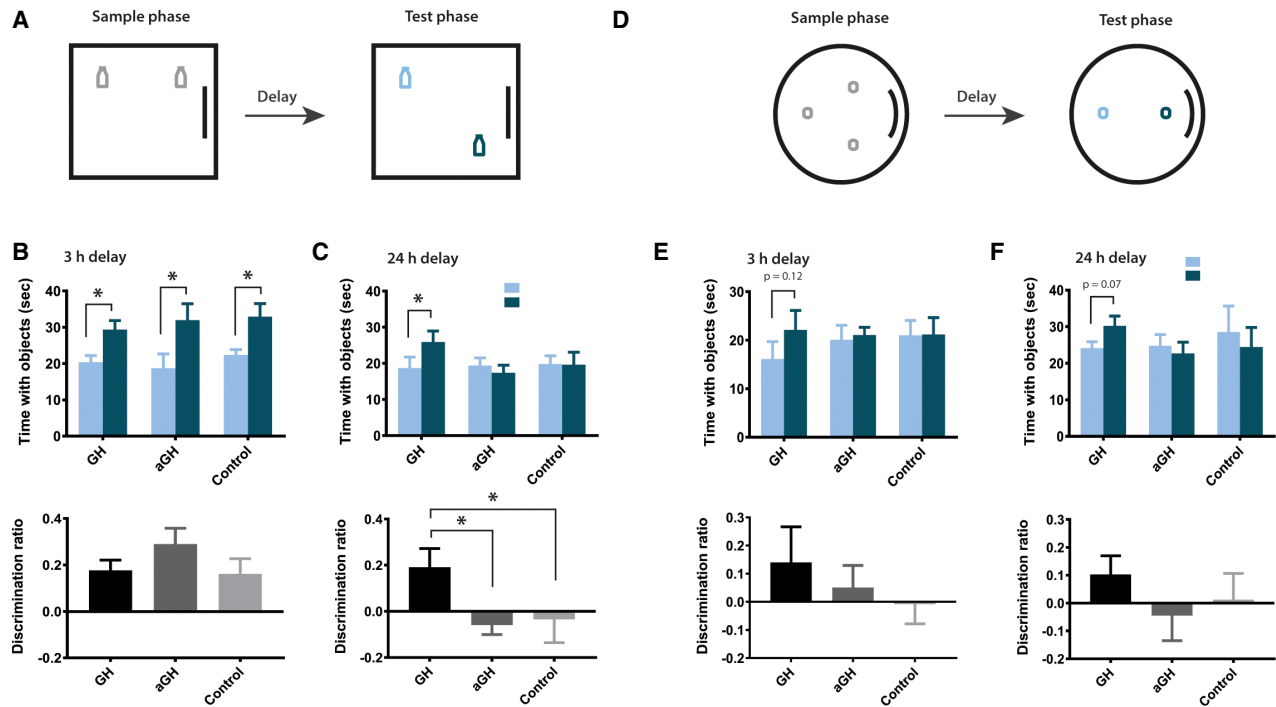
Figure 5. Growth hormone (GH) increases the preference for novel locations. (*A–C*) Easy version of the spontaneous location recognition (SLR) task using a square box with objects placed in the corners. New objects and pseudorandomized corners were used for each trial. (*B*) (*Upper* panel) After a 3-h delay, all groups spent significantly more time with the displaced object compared to the object in the familiar location (*upper* panel, paired *t*-tests, $P < 0.05$). (*Lower* panel) Comparison of discrimination ratio revealed no group differences (ANOVA $F_{(2,25)} = 1.16$, n.s., $n = 8$ GH, $n = 8$ antagonizing GH (aGH), $n = 13$ controls). (*C*) (*Upper* panel) Using a 24-h delay, only the GH treated animals explored the novel location significantly more than the familiar location ($t_{(7)} = 2.56$, $P < 0.05$.). (*Lower* panel) The GH rats also had a significantly higher discrimination ratio than the other two groups (ANOVA $F_{(2,26)} = 3.36$, $P = 0.05$, post-hoc contrasts $t_{(26)} = 2.59$, $P = 0.016$, as compared to controls and animals treated with aGH. (*D–F*) Second variation of the SLR task, using a circular arena with three objects in the sample phase. After the delay, the location of two objects were merged into one novel location. (*E,F*) (*Upper* panels) Only the GH group tended to explore the novel object location more, but not significantly (3 h delay condition: paired *t*-test, $t_{(7)} = 0.12$, 24 h delay condition: *t*-test $t_{(7)} = 0.07$). (*Lower* panels) ANOVA of the discrimination ratio showed no significant group differences ($P > 0.5$).

sample trial, with the 24 h delay (ANOVA $F_{(3,54)} = 1.18$, n.s.). Also, to rule out bias in the exploration data, we compared the exploration of the object location that would later remain in constant position, compared with the object location that would later be displaced. During the sample phase, there was no difference between these object locations (Fig. 6D–F; two-way ANOVAs n.s.).

For comparison between groups, we expressed the preference for novel/familiar location as a discrimination ratio from −1 to 1 (see Materials and Methods), which showed no effect of group in this easiest version of the SLR task (Fig. 5B lower panel; one-way ANOVA $F_{(2,25)} = 1.16$, n.s.). The discrimination ratio was also used to check that unoperated controls ($n = 6$) and AAV controls ($n = 7$) did not differ on any of the SLR tasks (*t*-tests, all P values >0.5) before the control groups were merged for all further statistics.

Next, we increased task difficulty by extending the delay between sample and test to 24 h. In the test phase, only the GH treated animals preferred to explore the object placed in the novel location (Fig. 5C upper panel; 25.9 ± 3.1 sec with novel, 18.7 ± 3.6 sec with familiar location; ($t_{(7)} = 2.56$, $P < 0.05$). The aGH and control groups spent equal amounts of time exploring the objects in both the novel and familiar locations (aGH: $t_{(7)} = 1.23$, n.s., control $t_{(12)} = 0.01$, n.s.). One-way ANOVA of the discrimination ratio (Fig. 5C lower panel; $F_{(2,26)} = 3.36$, $P = 0.05$) revealed a significant effect of group (discrimination ratio = 0.19 for GH, 0.06 for aGH, and −0.03 for control). Subsequent orthogonal comparisons showed that the aGH and control group did not differ ($t_{(26)} = 0.12$, n.s.), while the GH group performed above the other two groups ($t_{(26)} = 2.59$, $P < 0.05$).

In the last version of the SLR task, task difficulty was further increased by letting the rats explore three identical object in a circular familiar environment (Fig. 5D). In the test phase, two of the locations were merged to one novel location, so that only two identical copies of the objects were used. One object location remained constant (familiar location). As before, all the groups explored the objects equally in the sample phase (Fig. 6G–I, two-way ANOVAs n.s.). After a 3-h delay, only the GH rats tended to explore the novel object location more than the familiar location, but the effect was not statistically significant (Fig. 5E upper panel, one-tailed paired *t*-tests, GH $t_{(7)} = 1.27$, $P = 0.12$; aGH $t_{(7)} = 0.30$, $P = 0.38$; controls $t_{(12)} = 0.04$, $P = 0.48$). The discrimination ratio was not different between the groups (Fig. 5E lower panel, one-way ANOVA $F_{(2,26)} = 0.70$, n.s.). Last, we used a task setup with 24 h delay and a smaller distance between locations B and C (that would be merged). The GH group again showed a tendency to explore the novel object location more than the familiar object location, although the result did not reach statistical significance (Fig. 5F upper panel, one-tailed paired *t*-tests, GH group $t_{(7)} = 1.69$, $P = 0.07$; aGH $t_{(7)} = 0.20$, $P = 0.42$; controls $t_{(5)} = 0.16$, $P = 0.44$). The discrimination ratio was not different between groups (Fig. 5F lower panel, one-way ANOVA $F_{(2,19)} = 0.43$, n.s.).

Discussion

We have shown that relational memory is influenced by local levels of GH in the dorsal hippocampus. Antagonizing the GH
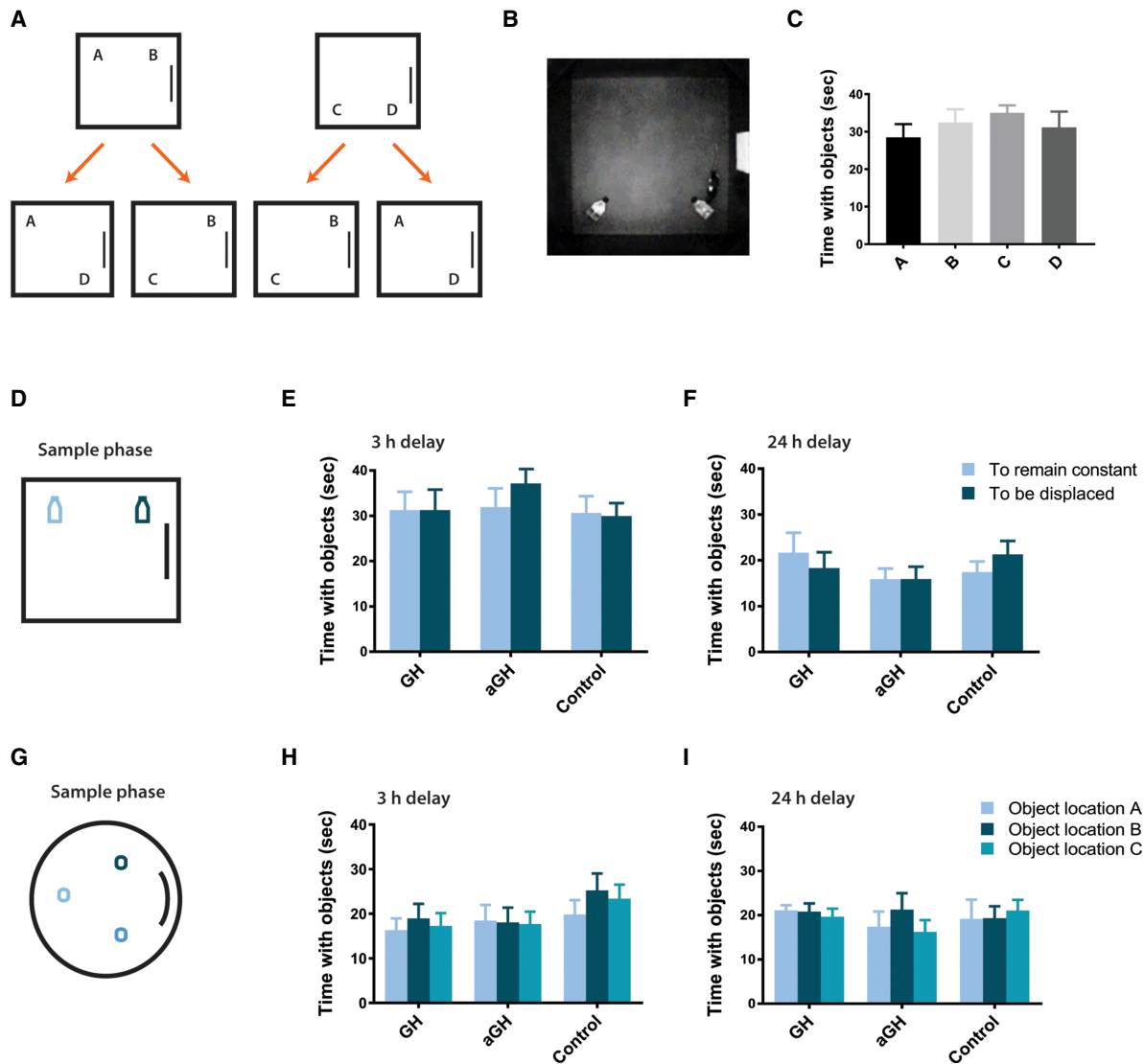
Figure 6. Exploration times with objects during the sample phase in the spontaneous recognition of location (SLR) tasks show no differences between the groups. (*A*) Randomized design for the SLR task with square box: During the sample phase (panel above), objects were placed in corners *A* and *B* or *C* and *D*. During later testing, one object was displaced as indicated by orange arrows (panel below). (*B*) Example frame from video camera when a rat explored an object in corner D during the sample phase. (*C*) Object exploration time for each corner during the sample phase showed no bias for corner. (*D*) Example of sample phase for the square arena. One object location (light blue) is to remain constant, and one object location (dark blue) is to be displaced upon later testing. The objects were identical. (*E,F*) Object exploration times for the object locations to remain in constant position (familiar) versus the object locations to be displaced, during the first 3 min of the sample phase. Two-way ANOVAs showed no effect of object location $F_{(1,26)} = 0.04$, n.s. and no Group × Location interaction $F_{(2,26)} = 0.68$, n.s., before the 3 h delay (*E*) or before the 24 h delay (*F*; two-way ANOVAs effect of object location $F_{(1,26)} = 0.06$, n.s. and Group × Location interaction $F_{(2,26)} = 1.84$, n.s.). (*G*) Sample phase for the circular arena. One object location is to remain constant (*A*, light blue), while the two other object locations (*B*, dark blue and *C*, blue) are to be displaced upon later testing. All the objects were identical. (*H,I*) Object exploring times for the three objects *A*, *B*, and *C* during the three first minutes of the sample phase in the circular arena. Two-way ANOVAs showed no effect of object location $F_{(2,52)} = 0.60$, n.s. and no Group × Location interaction $F_{(4,52)} = 0.32$, n.s.), before the 3 h delay (*H*) or before the 24 h delay (*I*; two-way ANOVAs effect of object location $F_{(2,38)} = 0.57$, n.s. and Group × Location interaction $F_{(4,38)} = 1.05$, n.s.).

receptor resulted in poorer memory performance in the water maze, a lower density of CA1 dendritic spines, and a lower percentage of immature spines. On the other hand, elevation of hippocampal GH levels was associated with higher density of dendritic spines, more immature spines, and enhanced memory in a single-trial SLR task under one of the test conditions. Our results suggest that GH is a neuromodulator that enhances learning capacity by affecting the dendritic spines (von Bohlen Und Halbach 2009). Several studies have reported cognitive impairments in cases of sys-

temic GH deficiency, and cognitive improvement after systemic GH replacement (Åberg 2010; Nyberg and Hallberg 2013; Ashpole et al. 2015). Our study provides important evidence for a common underlying assumption in these studies; namely that the effect on cognition, and in particular on memory, is mediated by the hippocampus. Extra-hippocampal mechanisms exist, for example in the amygdala (Meyer et al. 2014) and the prefrontal cortex (Enhamre et al. 2012), and the relative importance of GH in each brain region is still elusive.

Effects of the viral treatments

To verify the efficacy of the treatments used in this study, we analyzed the downstream phosphorylation of Stat5 (Fig. 2), which is a common method for measuring GH receptor activation (Furigo et al. 2017). The method successfully showed the expected increase in receptor activation in the GH group. However, the aGH group only showed a trend toward lower p-Stat5 count, not statistically significant from control rats. The measured outcome in spine density and behavior nevertheless indicated that the virus worked as intended, and we have considered several possible explanations for the lack of statistically significant change in p-Stat5 count. First, a floor effect is likely. It is well known that p-Stat5 as indicator of GH receptor activation is hard to observe without a significant GH injection/stimulation immediately before sacrifice and staining. A chronic blockade of GH receptors by the mutated GH would therefore not necessarily lower the overall receptor activation in the hippocampus, but rather prevent proper activation of the receptor during critical periods of learning. This is also consistent with results from pilot experiments in our laboratory using a five-fold higher virus dose (Supplemental Fig. 3). Second, the several weeks of overexpression of GH and aGH could have initiated downstream compensatory mechanisms or caused other parts of the network to change. Although we believe that the transfected cells in the injected area CA1 were principally responsible for the changes observed in this study, we know that AAV transfections easily spread to the DG. We therefore cannot claim that our effect was restricted to the CA1 only, as we also report GFP labeled neurons in CA3 and DG. In addition, GH is found to have both autocrine and paracrine effects (Gisabella et al. 2016), which means that GH could influence neighboring cells or other parts of the hippocampus as well as the transfected cells. Other genetic tools may allow experiments that decipher the relative contribution of GH in each hippocampal subarea. The fact that we still see behavioral and morphological effects after several weeks of chronic GH manipulation in only a part of the dorsal hippocampus suggests that the role of GH is important and could even be underestimated by the presented results. A larger transfection was avoided because of the risk of epilepsy and excitotoxic cell damage.

What are the mechanisms involved in hippocampal GH modulation?

To our knowledge, our report is the first to show that a direct GH manipulation in the hippocampus correlates with both behavioral and morphological changes. We found that GH enhances spine density while aGH reduces the spine density, but also report that aGH reduces the amount immature spines, important for learning and synaptic plasticity (Berry and Nedivi 2017). On the other hand, the GH rats had a lower percentage of mature spines and more immature spines, which indicate that the network plasticity is high. Spine formation is a morphological substrate for LTP, which is suggested to be the cellular mechanism behind learning and memory (Matsuzaki 2007). Previous studies have described the effects on spine density after the systemic elevation of ghrelin (Diano et al. 2006) and IGF2 in APP mice (Pascual-Lucas et al. 2014).

We cannot conclude that spine density is the only mechanism involved to alter learning and memory when GH levels are manipulated. For example, there is evidence implying the N-methyl-D-aspartate (NMDA) receptor, crucial for both water maze and object recognition tasks (Nakazawa et al. 2004; Warburton et al. 2013). Electrophysiological studies in vitro show that GH directly modulates glutamatergic synaptic transmission in the CA1 subfield of the hippocampus. Acute GH application in CA1 brain slices enhances both isolated NMDA and AMPA receptor field excitatory postsynaptic potentials (fEPSPs) in young and old rats (Mahmoud and Grover 2006; Molina et al. 2012, 2013). GH affects synaptic transmission in the absence of presynaptic changes, indicating postsynaptic changes responsible for the detected fEPSPs (Molina et al. 2012). Exogenous GH increases the expression of NMDA receptor subunit NR2B in young adult rats, thus changing the NR2A/NR2B ratio (Le Greves et al. 2002). Changing the ratio of these subunits alters the Ca^{2+} regulation, which can enhance LTP and synaptic plasticity (Nyberg and Hallberg 2013). Future studies should focus on the longitudinal dynamics of the GH-dependent changes, as in vivo imaging of spine dynamics indicate that increases in spine density are followed by a phase of elimination (Xu et al. 2009).

The relative contribution of the other components in the GH-axis, like ghrelin and/or the insulin-like growth factor (IGF)1 and 2, is also not well understood. IGF1 enhances adult neurogenesis by increasing the number of progenitor cells in the subgranular layer of DG (Åberg 2010), while IGF2 administration in the hippocampus improves memory consolidation (Chen et al. 2011), and reverses synaptic deficits in mice modeling Alzheimer's disease. Local IGF2 in the hippocampus has also been shown to promote spine formation (Pascual-Lucas et al. 2014). On the other hand, GH may improve hippocampal memory independently on IGF1 and IGF2, as patch-clamp studies indicate that GH directly enhances neural plasticity by increasing excitatory transmission in CA1 (Molina et al. 2012). To fully understand the impact GH in the hippocampus, further experiments are required to investigate effects of GH in the entire hippocampus, as well as the importance of the downstream processes.

Does growth hormone therapy require a deficiency to work?

The GH group performed better than controls only in one task setting, the 24 h delay square box SLR task. To enhance the performance above that of healthy control animals, some kind of residual potential in the organism may be necessary. This could happen in laboratory animals living under unstimulating or stressful conditions. However, as our rats were housed in an enriched environment and handled extensively before training, the residual potential for increasing the memory capacity by GH could be minimal. This may explain why the impact of GH in our study was not larger. This interpretation is in line with papers describing the rescue effects after GH treatment under conditions of distress or disease. For example, systemic GH treatment has been shown to restore normal cognitive function after sleep deprivation (Kim et al. 2010). Recombinant human GH in hypophysectomized male Sprague Dawley rats is reported to improve spatial memory of the hormone-ablated rats (Le Greves et al. 2006), which in a similar study was dose-dependent (Kwak et al. 2009). Rescue of the hippocampal GH levels is probably a key mechanism in these studies, as GH gene therapy in the hippocampus, an approach similar to ours, was shown to restore hippocampal memory function to normal levels after stress (Vander Weele et al. 2013). In humans, GH treatments in children with GH deficiency, or in older adults, have resulted in some cognitive improvement (Maruff and Falleti 2005; Baker et al. 2012). Another possible explanation why the GH group did not perform above controls in the water maze, is that the intensive training makes the task more sensitive to memory persistence than to memory acquisition.

Clinical significance of growth hormone in the aging brain

For memory to serve as a useful guide in decision-making, we need a combination of memory that maintains stable information (persistence) combined with the ability to forget and replace information (transience) (Richards and Frankland 2017). This perspective is useful when interpreting our data, rather than a classical

acquisition–retrieval perspective, and relates the data to everyday life. The aGH group showed a deficit in memory persistence on day 6, although at later testing they performed at the same level as controls. Perhaps their deficit was mainly in memory transience, the flexibility that allows rapid adaptation to new information, as they needed longer to relearn a novel goal location. This view fits with the notion that the GH group tended to search for both goal locations on the very last water maze probe trial, and also showed the greatest ability in the SLR tasks. The SLR tasks were performed with novel objects in the same room on subsequent days, challenging their pattern separation abilities as well as memory transience.

It is tempting to speculate that GH deficiency in the aging brain could be associated with a lower capacity for memory transience and a resistance to remodulate already acquired memories. Cementing behavior in adulthood could in general be an advantageous mechanism, preventing the common successful behavior to be overwritten by insignificant experience. Beneficial cognitive effects of GH treatment have been documented for aged animals and humans in several studies (Bartke 2008; Baker et al. 2012; Sonntag et al. 2012). GH is considered to be a replacement therapy, as adult GH levels drop dramatically in aging along with GH binding sites (Lai et al. 1993; Lobie et al. 1993), and GH is barely detectable after age 60 in some humans (Toogood and Shalet 1998). As systemic treatments may have severe side effects, especially in oncogenesis, a targeted approach to restore GH levels in the brain should be researched. Understanding the impact of GH in memory and learning may not only benefit GH deficient patients, but also all individuals that experience cognitive decline during normal aging.

Materials and Methods

Animals
In total, 44 adult male Long-Evans rats (Charles River, Italy) were used in this study, of which 37 animals were subjected to surgery (300–430 g at the time of surgery) and seven were left unoperated. For the animals receiving surgeries, 27 animals were used for behavioral assessment, while 10 rats were used for spine density analysis only. All the rats were housed in pairs in a controlled enriched environment, with constant humidity ($55 \pm 5\%$), temperature ($21 \pm 1°C$), and a 12-h light cycle (lights on at 7 p.m.). Food and water were available ad libitum. All experimental protocols followed the European Community Council Directive 2010/63, the Norwegian Experiments on Animals Act, and were approved by the Norwegian Animal Research Authority before initiation. Surgeries and the following behavioral assessments were done in batches of five to seven animals, each containing representatives for all three groups (GH, aGH, and control).

Viral vectors
Three recombinant adeno-associated viruses (rAAVs) 1/2 chimeric pseudotypes were used to either overexpress GH and GFP, mutated antagonizing (mutated) GH (aGH) and GFP, or GFP only (generous gift from Ki Ann Goosens, MIT). The construction of the viral vectors is described in more detail in Meyer et al. (2014), while a summary is presented here: Three cassettes were synthesized (Epoch Life Science), including one cassette containing the coding region of the rat *GH* gene (GeneBank Accession number U62779.1). Another cassette contained the rat *GH* gene with a single amino acid substitution at position 120 (*rGH-G120R*) to produce mutant GH protein with antagonist activity on the GH receptor. Both the cassettes contained internal ribosome entry site (IRES) and GFP. The third cassette only contained IRES and GFP. The cassettes were flanked by EcoRI and BGIII, and subcloned into pFB-AAV-CMV-SC40pa (V032) AAV gateway plasmid from Virotek (Hayward, CA), with AAV1/2 chimeric pseudotyping, yielding the three constructs: pAAV-CMV-GH-IRES-GFP, pAAV-CMV-aGH-IRES-GFP, and pAAV-CMV-IRES-GFP. The puri-

fied viruses were suspended in PBS, making the titers 2.46×10^{12} vg/mL for the control and GH AAV, and 2.42×10^{12} vg/mL for the aGH AAV.

Stereotaxic surgeries
All the surgeries were conducted under analgesia and deep isoflurane gas anesthesia. The animals ($n = 37$) were weighed and fully anesthetized in an induction chamber, before being placed on a heating plate (Agnthos; 37°C) on a stereotaxic frame (David Kopf Instruments). Buprenorphine (0.05 mg/kg) and Meloxicam (2 mg/kg) were given subcutaneously as analgesics, both before surgery and postsurgery. Simplex eye ointment was applied on the eyes to prevent dehydration. Nontraumatic ear bars positioned at the bones in the ear cavity were used to fixate the head. During surgery, the isoflurane concentration was adjusted according to reflexes, respiration rate, and oxygen saturation (Kent Scientific). Before incision, the skin was disinfected with 70% ethanol. The skin was cut open and holes were drilled at the appropriate locations on each hemisphere. Rats were randomly assigned to receive either pAAV-CMV-GH-IRES-GFP, pAAV-CMV-aGH-IRES-GFP, or pAAV-CMV-IRES-GFP. The viruses were injected with a sterile 2 µL Hamilton Syringe (Hamilton Company) using a pressure pump (KD Scientific). The rats received four injections of 0.4 µL virus solution (0.2 µL/min) in each hemisphere in the dorsal hippocampal area CA1 according to the injection coordinates calculated anteroposteriorly (AP), mediolaterally (ML) from bregma, and dorsoventrally (DV) from dura: AP −3.0 mm, ML ± 1.2 mm, DV 2.3 mm; AP −3.5 mm, ML ± 2.2 mm, DV 2.2 mm; AP −4.0 mm, ML ± 2.4 mm, DV 2.4 mm; AP −4.4 mm, ML ± 3.5 mm, DV 2.8 mm. The needle was left at the site of injection for 5 min after each injection to allow diffusion of the virus before slow retraction. After the last injection, the skin was sutured and the animals were allowed to recover with a warm water bottle in their home cages.

Behavioral tasks

Spontaneous location recognition tasks
Two weeks after surgery, 22 operated and seven unoperated rats were habituated to an empty open field arena (1×1 m with 60 cm walls), 15 min per day for 5 d. A white cue card (21.0×29.7 cm) on one of the black walls served as a local cue. Items in the room (cabinets, boxes) served as distal cues and remained constant throughout the experiment. After habituation, all rats participated in two main variations of the task (square and circle arenas), consisting of a sample phase and a test phase separated by either 3 or 24 h. In the sample phase, the rats explored novel objects which were secured in place by blue-tack. In the following test phase, one object was put in a novel location while the other object remained in the familiar location, both secured by blue-tack, and using copies of identical objects to avoid transfer of smell. The animal's natural preference for exploring the displaced object was manually scored by two blind observers in Ethovision XT 11.5, using video tracking. Object exploration was defined as rat directing its nose toward the object at a distance of 2 cm or less. Standing on the object with the nose clearly pointing away from the object was not counted as object exploration. The preference for the displaced object was calculated by the discrimination ratio, that is, the difference in time spent with the object placed in the novel location and the object in the familiar location divided on the sum of the time spent with both of them. A score of 1 indicates that the animals only spent time near the object in the novel location, while a score of −1 means that the animals visited only the familiar object location. We analyzed the first 3 min of the 5 min test phase as the animals explored the objects the most during these first minutes. This is in line with reports from other labs using this task to describe the preference for displaced objects during the first 2–3 min (Dix and Aggleton 1999; Larkin et al. 2014). To avoid familiarization to the objects, the animals explored new sets of unique objects in each task variation. Between trials, the arena and the objects were cleaned with water and 70% ethanol. Objects that were used included blue tea light holders (6.5 cm in diameter × 3.5 cm

height), serum bottles (7.5 cm × 3.5 cm × 15 cm) with blue corks, clear plastic water bottles (6 cm in diameter × 14 height) covered with green tape, Falcon 50 mL Centrifuge tubes (3.5 cm in diameter × 11.5 height), and standing petri dishes on metal plates covered in green, blue, and orange tape (about 2 × 6 × 9 cm).

In the square version of the task, the familiar 1 × 1 m open field box was used. In the sample phase, two identical objects were located in random corners next to each other 10 cm from the walls (Figs. 5A, 6A–F). In the test phase, one object was relocated to the diagonally and opposing corner of the box. The animals were allowed to explore the arena with the objects for 5 min in the test phase before they were put back to their home cages. To avoid exploration bias for any preferred corner in the data, all four corners were used in each condition (familiar/novel) an equal amount of times in a pseudorandomized order (Fig. 6A,C). The order of task variations was square 3 h, square 24 h, circle 3 h, and circle 24 h.

In the circular version of the task, animals were first given one habituation session for 10 min to the cylindrical arena (90 cm in diameter, 60 cm high) before they were put back to their home cages. In the sample phase, three identical objects (A, B, C) were located in the arena (Fig. 6G–I). Object A was located the furthest away from the other two objects. The rats were allowed to explore the three objects for 10 min in the sample phase before they were moved back to their home cages. After a delay of 3 or 24 h, the animals were put back to the circular arena for the test phase. For the task with 3 h delay, the objects in the sample phase were situated in largest distance to each other (120° between object A and the other two objects, object B and C), while for the most challenging condition, we used 24 h delay between trials and a smaller separation between the objects (40°). In the test phase, only two identical copies of the objects (A, D) were assessable (Fig. 5D). The object location for object A in the test phase was identical to the location for object A in the sample phase, making this a familiar location, while object D was placed between the former locations of the objects in the sample phase, objects B and C, resulting in a novel location.

Morris water maze task

Rats transfected with virus ($n = 27$) were trained in a water maze (2 m in diameter, filled with 50 cm opaque water, about 23°C), for five consecutive days to find a submerged platform located southwest (SW). Each training day consisted of eight trials. The trials were divided into two sessions of four trials each, separated by at least 3 h. The first trial of each day was a single reinforcement probe trial, in which the rats were searching for the hidden platform location for 60 sec before the platform was raised to an available position. Then, another 60 sec were provided for the rats to locate the platform. During the other seven trials of the day, the platform remained in the raised and available position, 1 cm below opaque water. If the rat failed to locate the platform within 120 sec, it was manually guided to the platform by the experimenter. After each trial, the rats were allowed to rest for 30 sec on the platform. The overall memory performance was measured during a probe trial on day 6. The starting positions (South, East, North, West) were counterbalanced across the trials. After each training session (four trials), the rats were put to dry under a heating lamp. One week after the last training session, the rats received an additional 2 d (day 12 and 13) of reversal training with the platform located in the quadrant opposite to the previous goal. Learning the new platform location was measured on the probe trial the subsequent day (day 14).

Balance test

After the water maze tasks, the animals were subjected to a balance beam test to rule out any motor or balance effects of the treatment which could influence the water maze performance. We used a 60 cm long and 3 cm broad ruler placed on plastic shelves, 40 cm high off ground. The animals were placed in the middle and left balancing on the ruler for maximum 1 min.

Perfusion and sectioning

All the rats were deeply anesthetized with isoflurane gas before given Buprenorphine (0.05 mg/kg) and a lethal dose of Pentobarbital (100 mg/kg). The rats were transcardially perfused with physiological PBS and then a 4% paraformaldehyde in PBS solution (pH 7.4) at 80 mL/min using a peristaltic pump (World Precision Instruments). The brains were submerged in a 4% paraformaldehyde solution for additional fixation before 2% dimethyl sulfoxide and 20% glycerol (DMSO) at 4°C. The rats used for spine analysis ($n = 10$) were perfused with ice-cold physiological PBS before brain tissue was stored in a 4% paraformaldehyde solution for 1 wk and then in dimethyl sulfoxide (DMSO) until the brain was sectioned. The brains were cut coronally on Leica CM1950 cryostat (Leica Biosystems), with 40 µm thick sections with six series, in which the first series was put directly on Super Frost glass slides for Cresyl violet (Nissl) staining (Sigma-Aldrich), while the other sections were put on DMSO for immunohistochemistry and stored at −20°C. The brains for spine analysis were cut in 100 µm thick sections and stored at 4°C.

Immunohistochemistry

To assess the viral transfection in the brains from all the animals used in behavioral testing, the GFP expression in the tissue was amplified using a free-floating immunohistochemistry protocol. The 40 µm thick sections were washed with 0.01 M PBS for 5 min repeated six times (later washed three times between the steps), before put on ice-cold methanol at −20°C for 10 min to disturb the integrity of the cell membrane. The sections were washed for 5 min three times. The sections were transferred to a blocking buffer (1% BSA, 0.2% Triton-X, in 0.01 M PBS) for 1 h, then incubated with primary antibody anti-Chicken GFP Polyclonal antibody, 1:2000 dilution (ThermoFischer # A10262) overnight at room temperature. Then, the sections were incubated in secondary antibody Goat anti-Chicken IgY Alexa Fluor 488, 1:200 dilution (ThermoFischer # A-11039) for 2 h and mounted using ProLong DAPI antifade (ThermoFischer # P36941). For the GFP immunohistochemistry of the 100 µm thick sections, the tissues were stained with primary and secondary antibodies for GFP as described above, but with longer blocking time (2 h), higher concentrations for the anti-Chicken GFP Polyclonal antibody (1:1000), and higher concentration (1:100) and longer incubation time (4 h) for the Goat anti-Chicken IgY Alexa Fluor 488.

For phosphorylated Signal transducer and activator of transcription 5 (p-Stat5) immunohistochemistry, representative sections from animals used in the behavioral tests were used ($n = 15$ in four GH rats, $n = 12$ in three aGH rats, $n = 12$ in three control rats). Sections were transferred to a blocking buffer with 5% normal goat serum (Sigma-Aldrich), and 0.3% Triton-X in 0.01 M PBS for 1 h, and incubated with primary antibody anti-Rabbit p-Stat5 (1:200 dilution, Cell Signal # 9314) overnight at 4°C. Consequently, the sections were incubated with secondary antibody anti-Rabbit IgG Alexa Fluor 546 Conjugate (1:200, Termofisher # A-11071) for 2 h and mounted using ProLong DAPI antifade (ThermoFischer #P36941). The fluorescence in the tissue was imaged by a fluorescence microscope Axio Zoom V.16 (Carl Zeiss). Positive p-Stat5 labeled DAPI cells were manually counted blinded for treatment in an area of 0.5 mm^2 per section in immediate proximity to the injection sites, using Zen 2 Lite Software.

Spine analysis

For analyzing the effects of the GH treatment on spine density, we looked at 100 µm thick sections after GFP immunohistochemistry and DAPI labeling in 10 rats ($n = 3$ GH, $n = 3$ aGH, $n = 4$ control). These sections were from animals that were not used in behavioral tests. Images of neurons were obtained from a confocal microscope Zeiss LSM 780 with ZEN 2012 black edition imaging software. An eGFP contrast filter and 488 nm wavelength argon laser were used to gather a Z-stack of laser scan images (1756 × 1756 pixels) averaged four times, with an average optimal Z distance at 0.6× optical zoom, and a 100× oil objective. The Z-stack images were analyzed with ImageJ (NIH). The resolution of the stack image

was increased by a factor of 3 in the X and Y directions with the Transform J Scale plug-in, and the spines were counted using the Cell Counter plug-in to manually mark spines. Spines from apical dendrites of CA1 pyramidal cells were defined as in the following review (von Bohlen Und Halbach 2009), and sampled between 100 and 200 µm from the pyramidal layer, where the density of the spines is relatively uniform (Megias et al. 2001), when the dendrites were clearly traceable. The spine density was averaged by dividing the number of spines on the length of the dendritic segment and calculated on cell level ($n = 64$ dendritic segments in 15 neurons from GH animals, $n = 75$ dendritic segments from 22 neurons in aGH animals, and $n = 49$ dendritic segments in eight neurons in control animals). The spines were further classified based on their morphology as either filopodia, immature or mature spines. All analysis was performed blind to the virus treatment, as K.G.H. performed the surgeries and histology, while A.O. and A.L. did the work on spine density measurement and classification.

Experimental design and statistical analysis

All of the data is presented as mean ± SEM. Statistical analysis was performed in SPSS (IBM Corporation) and MATLAB (Mathworks) with $\alpha = 0.05$. Water maze data was analyzed first by testing for effect of platform Zone and Group × Zone interaction by a two-way analysis of variance (ANOVA). If significant Group × Zone effects were found, time in the target platform zone was evaluated by one-way ANOVA followed by orthogonal comparisons between the groups. The data in the SLR tasks was analyzed using one-way ANOVA and paired t-test. For the histology, the p-Stat5 positive cells were analyzed using ANOVA followed by t-tests. Nonparametric tests (Jonckheere–Terpstra test, Mann–Whitney U) were chosen for spine density analysis due to lack of normal distribution in the data set and low number of animals, while spine classification was analyzed by ANOVA and post-hoc contrast t-tests. The position of the animals in the water maze was sampled using Dacq acquisition system (Axona Ltd). The performance in the task was calculated by measuring the mean latency to the platform location (sec), time in zone (sec), and plotting occupancy maps for heat map visualization of the swimming path in MATLAB. Videos from the SLR tasks were recorded and analyzed using EthoVision Software (Noldus). Graphs for illustrations were made using GraphPad Prism version 7.09 (GraphPad Software).

Acknowledgments

References

Åberg D. 2010. Role of the growth hormone/insulin-like growth factor 1 axis in neurogenesis. *Endocr Dev* **17:** 63–76. doi:10.1159/000262529

Åberg ND, Brywe KG, Isgaard J. 2006. Aspects of growth hormone and insulin-like growth factor-I related to neuroprotection, regeneration, and functional plasticity in the adult brain. *ScientificWorldJournal* **6:** 53–80. doi:10.1100/tsw.2006.22

Albarran-Zeckler RG, Brantley AF, Smith RG. 2012. Growth hormone secretagogue receptor (GHS-R1a) knockout mice exhibit improved

spatial memory and deficits in contextual memory. *Behav Brain Res* **232:** 13–19. doi:10.1016/j.bbr.2012.03.012

Ashpole NM, Sanders JE, Hodges EL, Yan H, Sonntag WE. 2015. Growth hormone, insulin-like growth factor-1 and the aging brain. *Exp Gerontol* **68:** 76–81. doi:10.1016/j.exger.2014.10.002

Baker LD, Barsness SM, Borson S, Merriam GR, Friedman SD, Craft S, Vitiello MV. 2012. Effects of growth hormone-releasing hormone on cognitive function in adults with mild cognitive impairment and healthy older adults: results of a controlled trial. *Arch Neurol* **69:** 1420–1429. doi:10.1001/archneurol.2012.1970

Bartke A. 2008. Growth hormone and aging: a challenging controversy. *Clin Interv Aging* **3:** 659–665. doi:10.2147/CIA.S3697

Basu A, McFarlane HG, Kopchick JJ. 2017. Spatial learning and memory in male mice with altered growth hormone action. *Horm Behav* **93:** 18–30. doi:10.1016/j.yhbeh.2017.04.001

Bekinschtein P, Kent BA, Oomen CA, Clemenson GD, Gage FH, Saksida LM, Bussey TJ. 2013. BDNF in the dentate gyrus is required for consolidation of "pattern-separated" memories. *Cell Rep* **5:** 759–768. doi:10.1016/j.celrep.2013.09.027

Berry KP, Nedivi E. 2017. Spine dynamics: are they all the same? *Neuron* **96:** 43–55. doi:10.1016/j.neuron.2017.08.008

Birzniece V, Sata A, Ho KK. 2009. Growth hormone receptor modulators. *Rev Endocr Metab Disord* **10:** 145–156. doi:10.1007/s11154-008-9089-x

Brun VH, Ytterbø K, Morris RG, Moser MB, Moser EI. 2001. Retrograde amnesia for spatial memory induced by NMDA receptor-mediated long-term potentiation. *J Neurosci* **21:** 356–362. doi:10.1523/JNEUROSCI.21-01-00356.2001

Burton KA, Kabigting EB, Clifton DK, Steiner RA. 1992. Growth hormone receptor messenger ribonucleic acid distribution in the adult male rat brain and its colocalization in hypothalamic somatostatin neurons. *Endocrinology* **131:** 958–963. doi:10.1210/endo.131.2.1353444

Chen WY, Wight DC, Wagner TE, Kopchick JJ. 1990. Expression of a mutated bovine growth hormone gene suppresses growth of transgenic mice. *Proc Natl Acad Sci* **87:** 5061–5065. doi:10.1073/pnas.87.13.5061

Chen WY, Wight DC, Mehta BV, Wagner TE, Kopchick JJ. 1991. Glycine 119 of bovine growth hormone is critical for growth-promoting activity. *Mol Endocrinol* **5:** 1845–1852. doi:10.1210/mend-5-12-1845

Chen DY, Stern SA, Garcia-Osta A, Saunier-Rebori B, Pollonini G, Bambah-Mukku D, Blitzer RD, Alberini CM. 2011. A critical role for IGF-II in memory consolidation and enhancement. *Nature* **469:** 491–497. doi:10.1038/nature09667

Cobb S, Lawrence JJ. 2010. Neuromodulation of hippocampal cells and circuits. In *Hippocampal microcircuits* (ed. Vassils Cutsurdis BG, Cobb S, Vida I), pp. 617. Springer, New York, USA.

Deijen JB, de Boer H, van der Veen EA. 1998. Cognitive changes during growth hormone replacement in adult men. *Psychoneuroendocrinology* **23:** 45–55. doi:10.1016/S0306-4530(97)00092-9

Diano S, Farr SA, Benoit SC, McNay EC, da Silva I, Horvath B, Gaskin FS, Nonaka N, Jaeger LB, Banks WA, et al. 2006. Ghrelin controls hippocampal spine synapse density and memory performance. *Nat Neurosci* **9:** 381–388. doi:10.1038/nn1656

Dix SL, Aggleton JP. 1999. Extending the spontaneous preference test of recognition: evidence of object-location and object-context recognition. *Behav Brain Res* **99:** 191–200. doi:10.1016/S0166-4328(98)00079-5

Donahue CP, Kosik KS, Shors TJ. 2006. Growth hormone is produced within the hippocampus where it responds to age, sex, and stress. *Proc Natl Acad Sci* **103:** 6031–6036. doi:10.1073/pnas.0507776103

Eichenbaum H. 2017. The role of the hippocampus in navigation is memory. *J Neurophysiol* **117:** 1785–1796. doi:10.1152/jn.00005.2017

Enhamre E, Carlsson A, Grönbladh A, Watanabe H, Hallberg M, Nyberg F. 2012. The expression of growth hormone receptor gene transcript in the prefrontal cortex is affected in male mice with diabetes-induced learning impairments. *Neurosci Lett* **523:** 82–86. doi:10.1016/j.neulet.2012.06.050

Furigo IC, Metzger M, Teixeira PD, Soares CR, Donato J Jr. 2017. Distribution of growth hormone-responsive cells in the mouse brain. *Brain Struct Funct* **222:** 341–363. doi:10.1007/s00429-016-1221-1

Gisabella B, Farah S, Peng X, Burgos-Robles A, Lim SH, Goosens KA. 2016. Growth hormone biases amygdala network activation after fear learning. *Transl Psychiatry* **6:** e960. doi:10.1038/tp.2016.203

Grönbladh A, Johansson J, Nöstl A, Nyberg F, Hallberg M. 2013. GH improves spatial memory and reverses certain anabolic androgenic steroid-induced effects in intact rats. *J Endocrinol* **216:** 31–41. doi:10.1530/JOE-12-0315

Kim E, Grover LM, Bertolotti D, Green TL. 2010. Growth hormone rescues hippocampal synaptic function after sleep deprivation. *Am J Physiol Regul Integr Comp Physiol* **298:** R1588–R1596. doi:10.1152/ajpregu.00580.2009

Kwak MJ, Park HJ, Nam MH, Kwon OS, Park SY, Lee SY, Kim MJ, Kim SJ, Paik KH, Jin DK. 2009. Comparative study of the effects of different growth hormone doses on growth and spatial performance of

hypophysectomized rats. *J Korean Med Sci* **24:** 729–736. doi:10.3346/jkms.2009.24.4.729

Lai Z, Roos P, Zhai O, Olsson Y, Fhölenhag K, Larsson C, Nyberg F. 1993. Age-related reduction of human growth hormone-binding sites in the human brain. *Brain Res* **621:** 260–266. doi:10.1016/0006-8993(93)90114-3

Larkin MC, Lykken C, Tye LD, Wickelgren JG, Frank LM. 2014. Hippocampal output area CA1 broadcasts a generalized novelty signal during an object-place recognition task. *Hippocampus* **24:** 773–783. doi:10.1002/hipo.22268

Le Greves M, Steensland P, Le Greves P, Nyberg F. 2002. Growth hormone induces age-dependent alteration in the expression of hippocampal growth hormone receptor and N-methyl-D-aspartate receptor subunits gene transcripts in male rats. *Proc Natl Acad Sci* **99:** 7119–7123. doi:10.1073/pnas.092135399

Le Grevès M, Zhou Q, Berg M, Le Grevès P, Fhölenhag K, Meyerson B, Nyberg F. 2006. Growth hormone replacement in hypophysectomized rats affects spatial performance and hippocampal levels of NMDA receptor subunit and PSD-95 gene transcript levels. *Exp Brain Res* **173:** 267–273. doi:10.1007/s00221-006-0438-2

Leutgeb JK, Leutgeb S, Moser MB, Moser EI. 2007. Pattern separation in the dentate gyrus and CA3 of the hippocampus. *Science* **315:** 961–966. doi:10.1126/science.1135801

Li E, Kim DH, Cai M, Lee S, Kim Y, Lim E, Hoon Ryu J, Unterman TG, Park S. 2011. Hippocampus-dependent spatial learning and memory are impaired in growth hormone-deficient spontaneous dwarf rats. *Endocr J* **58:** 257–267. doi:10.1507/endocrj.K11E-006

Lobie PE, García-Aragón J, Lincoln DT, Barnard R, Wilcox JN, Waters MJ. 1993. Localization and ontogeny of growth hormone receptor gene expression in the central nervous system. *Brain Res Dev Brain Res* **74:** 225–233. doi:10.1016/0165-3806(93)90008-X

Lobie PE, Zhu T, Graichen R, Goh EL. 2000. Growth hormone, insulin-like growth factor I and the CNS: localization, function and mechanism of action. *Growth Horm IGF Res* **10:** S51–S56. doi:10.1016/S1096-6374(00)80010-6

Mahmoud GS, Grover LM. 2006. Growth hormone enhances excitatory synaptic transmission in area CA1 of rat hippocampus. *J Neurophysiol* **95:** 2962–2974. doi:10.1152/jn.00947.2005

Maruff P, Falleti M. 2005. Cognitive function in growth hormone deficiency and growth hormone replacement. *Horm Res* **64:** 100–108. doi:10.1159/000089325

Matsuzaki M. 2007. Factors critical for the plasticity of dendritic spines and memory storage. *Neurosci Res* **57:** 1–9. doi:10.1016/j.neures.2006.09.017

Megias M, Emri Z, Freund TF, Gulyás AI. 2001. Total number and distribution of inhibitory and excitatory synapses on hippocampal CA1 pyramidal cells. *Neuroscience* **102:** 527–540. doi:10.1016/s0306-4522(00)00496-6

Meyer RM, Burgos-Robles A, Liu E, Correia SS, Goosens KA. 2014. A ghrelin-growth hormone axis drives stress-induced vulnerability to enhanced fear. *Mol Psychiatry* **19:** 1284–1294. doi:10.1038/mp.2013.135

Molina DP, Ariwodola OJ, Linville C, Sonntag WE, Weiner JL, Brunso-Bechtold JK, Adams MM. 2012. Growth hormone modulates hippocampal excitatory synaptic transmission and plasticity in old rats. *Neurobiol Aging* **33:** 1938–1949. doi:10.1016/j.neurobiolaging.2011.09.014

Molina DP, Ariwodola OJ, Weiner JL, Brunso-Bechtold JK, Adams MM. 2013. Growth hormone and insulin-like growth factor-I alter hippocampal excitatory synaptic transmission in young and old rats. *Age (Dordr)* **35:** 1575–1587. doi:10.1007/s11357-012-9460-4

Morris RG, Garrud P, Rawlins JN, O'Keefe J. 1982. Place navigation impaired in rats with hippocampal lesions. *Nature* **297:** 681–683. doi:10.1038/297681a0

Moser MB, Trommald M, Andersen P. 1994. An increase in dendritic spine density on hippocampal CA1 pyramidal cells following spatial learning in adult rats suggests the formation of new synapses. *Proc Natl Acad Sci* **91:** 12673–12675. doi:10.1073/pnas.91.26.12673

Nakazawa K, McHugh TJ, Wilson MA, Tonegawa S. 2004. NMDA receptors, place cells and hippocampal spatial memory. *Nat Rev Neurosci* **5:** 361–372. doi:10.1038/nrn1385

Nieves-Martinez E, Sonntag WE, Wilson A, Donahue A, Molina DP, Brunso-Bechtold J, Nicolle MM. 2010. Early-onset GH deficiency results in spatial memory impairment in mid-life and is prevented by GH supplementation. *J Endocrinol* **204:** 31–36. doi:10.1677/JOE-09-0323

Nyberg F. 2000. Growth hormone in the brain: characteristics of specific brain targets for the hormone and their functional significance. *Front Neuroendocrinol* **21:** 330–348. doi:10.1006/frne.2000.0200

Nyberg F, Hallberg M. 2013. Growth hormone and cognitive function. *Nat Rev Endocrinol* **9:** 357–365. doi:10.1038/nrendo.2013.78

Ozcan AS. 2017. Filopodia: a rapid structural plasticity substrate for fast learning. *Front Synaptic Neurosci* **9:** 12. doi:10.3389/fnsyn.2017.00012

Palacios-Filardo J, Mellor JR. 2018. Neuromodulation of hippocampal long-term synaptic plasticity. *Curr Opin Neurobiol* **54:** 37–43. doi:10.1016/j.conb.2018.08.009

Pan W, Yu Y, Cain CM, Nyberg F, Couraud PO, Kastin AJ. 2005. Permeation of growth hormone across the blood-brain barrier. *Endocrinology* **146:** 4898–4904. doi:10.1210/en.2005-0587

Pascual-Lucas M, Viana da Silva S, Di Scala M, Garcia-Barroso C, González-Aseguinolaza G, Mulle C, Alberini CM, Cuadrado-Tejedor M, Garcia-Osta A. 2014. Insulin-like growth factor 2 reverses memory and synaptic deficits in APP transgenic mice. *EMBO Mol Med* **6:** 1246–1262. doi:10.15252/emmm.201404228

Ramis M, Sarubbo F, Sola J, Aparicio S, Garau C, Miralles A, Esteban S. 2013. Cognitive improvement by acute growth hormone is mediated by NMDA and AMPA receptors and MEK pathway. *Prog Neuropsychopharmacol Biol Psychiatry* **45:** 11–20. doi:10.1016/j.pnpbp.2013.04.005

Richards BA, Frankland PW. 2017. The persistence and transience of memory. *Neuron* **94:** 1071–1084. doi:10.1016/j.neuron.2017.04.037

Sathiavageeswaran M, Burman P, Lawrence D, Harris AG, Falleti MG, Maruff P, Wass J. 2007. Effects of GH on cognitive function in elderly patients with adult-onset GH deficiency: a placebo-controlled 12-month study. *Eur J Endocrinol* **156:** 439–447. doi:10.1530/eje.1.02346

Schneider-Rivas S, Rivas-Arancibia S, Vazquez-Pereyra F, Vázquez-Sandoval R, Borgonio-Pérez G. 1995. Modulation of long-term memory and extinction responses induced by growth hormone (GH) and growth hormone releasing hormone (GHRH) in rats. *Life Sci* **56:** PL433–PL441. doi:10.1016/0024-3205(95)00171-2

Shimizu E, Tang YP, Rampon C, Tsien JZ. 2000. NMDA receptor-dependent synaptic reinforcement as a crucial process for memory consolidation. *Science* **290:** 1170–1174. doi:10.1126/science.290.5494.1170

Sonntag WE, Csiszar A, deCabo R, Ferrucci L, Ungvari Z. 2012. Diverse roles of growth hormone and insulin-like growth factor-1 in mammalian aging: progress and controversies. *J Gerontol A Biol Sci Med Sci* **67:** 587–598. doi:10.1093/gerona/gls115

Studzinski AL, Barros DM, Marins LF. 2015. Growth hormone (GH) increases cognition and expression of ionotropic glutamate receptors (AMPA and NMDA) in transgenic zebrafish (Danio rerio). *Behav Brain Res* **294:** 36–42. doi:10.1016/j.bbr.2015.07.054

Sun LY, Bartke A. 2014. Tissue-Specific GHR Knockout Mice: metabolic Phenotypes. *Front Endocrinol (Lausanne)* **5:** 243. doi:10.3389/fendo.2014.00243

Sun LY, Al-Regaiey K, Masternak MM, Wang J, Bartke A. 2005. Local expression of GH and IGF-1 in the hippocampus of GH-deficient long-lived mice. *Neurobiol Aging* **26:** 929–937. doi:10.1016/j.neurobiolaging.2004.07.010

Toogood AA, Shalet SM. 1998. Ageing and growth hormone status. *Baillieres Clin Endocrinol Metab* **12:** 281–296. doi:10.1016/S0950-351X(98)80023-2

Vander Weele CM, Saenz C, Yao J, Correia SS, Goosens KA. 2013. Restoration of hippocampal growth hormone reverses stress-induced hippocampal impairment. *Front Behav Neurosci* **7:** 66. doi:10.3389/fnbeh.2013.00066

von Bohlen Und Halbach O. 2009. Structure and function of dendritic spines within the hippocampus. *Ann Anat* **191:** 518–531. doi:10.1016/j.aanat.2009.08.006

Warburton EC, Barker GR, Brown MW. 2013. Investigations into the involvement of NMDA mechanisms in recognition memory. *Neuropharmacology* **74:** 41–47. doi:10.1016/j.neuropharm.2013.04.013

Xu T, Yu X, Perlik AJ, Tobin WF, Zweig JA, Tennant K, Jones T, Zuo Y. 2009. Rapid formation and selective stabilization of synapses for enduring motor memories. *Nature* **462:** 915–919. doi:10.1038/nature08389

Zhao Z, Liu H, Xiao K, Yu M, Cui L, Zhu Q, Zhao R, Li GD, Zhou Y. 2014. Ghrelin administration enhances neurogenesis but impairs spatial learning and memory in adult mice. *Neuroscience* **257:** 175–185. doi:10.1016/j.neuroscience.2013.10.063